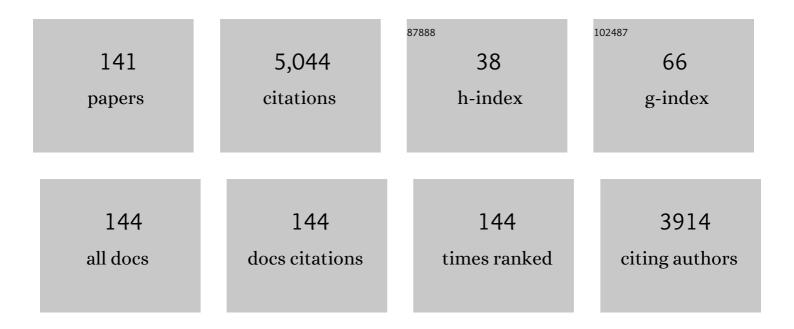
Carlos Jacinto

List of Publications by Year in descending order

Source: https://exaly.com/author-pdf/2922678/publications.pdf Version: 2024-02-01



#	Article	IF	CITATIONS
1	Subtissue Thermal Sensing Based on Neodymium-Doped LaF ₃ Nanoparticles. ACS Nano, 2013, 7, 1188-1199.	14.6	338
2	Intratumoral Thermal Reading During Photoâ€Thermal Therapy by Multifunctional Fluorescent Nanoparticles. Advanced Functional Materials, 2015, 25, 615-626.	14.9	274
3	Unveiling in Vivo Subcutaneous Thermal Dynamics by Infrared Luminescent Nanothermometers. Nano Letters, 2016, 16, 1695-1703.	9.1	265
4	Neodymiumâ€Doped LaF ₃ Nanoparticles for Fluorescence Bioimaging in the Second Biological Window. Small, 2014, 10, 1141-1154.	10.0	185
5	1.3 \hat{l} $\!\!\!\!^{1}\!\!\!\!^{4}$ m emitting SrF2:Nd3+ nanoparticles for high contrast in vivo imaging in the second biological window. Nano Research, 2015, 8, 649-665.	10.4	185
6	In Vivo Subcutaneous Thermal Video Recording by Supersensitive Infrared Nanothermometers. Advanced Functional Materials, 2017, 27, 1702249.	14.9	159
7	Thermal lens and Z-scan measurements: Thermal and optical properties of laser glasses – A review. Journal of Non-Crystalline Solids, 2006, 352, 3582-3597.	3.1	141
8	Lifetime-Encoded Infrared-Emitting Nanoparticles for <i>in Vivo</i> Multiplexed Imaging. ACS Nano, 2018, 12, 4362-4368.	14.6	138
9	CdTe Quantum Dots as Nanothermometers: Towards Highly Sensitive Thermal Imaging. Small, 2011, 7, 1774-1778.	10.0	127
10	Yb3+/Tm3+ co-doped NaNbO3 nanocrystals as three-photon-excited luminescent nanothermometers. Sensors and Actuators B: Chemical, 2015, 213, 65-71.	7.8	120
11	Nd3+ doped LaF3 nanoparticles as self-monitored photo-thermal agents. Applied Physics Letters, 2014, 104, 053703.	3.3	116
12	Self-monitored photothermal nanoparticles based on core–shell engineering. Nanoscale, 2016, 8, 3057-3066.	5.6	107
13	Neodymium-doped nanoparticles for infrared fluorescence bioimaging: The role of the host. Journal of Applied Physics, 2015, 118, .	2.5	102
14	In Vivo Early Tumor Detection and Diagnosis by Infrared Luminescence Transient Nanothermometry. Advanced Functional Materials, 2018, 28, 1803924.	14.9	83
15	LaF3 core/shell nanoparticles for subcutaneous heating and thermal sensing in the second biological-window. Applied Physics Letters, 2016, 108, .	3.3	78
16	In Vivo Ischemia Detection by Luminescent Nanothermometers. Advanced Healthcare Materials, 2017, 6, 1601195.	7.6	73
17	Ag ₂ S Nanoheaters with Multiparameter Sensing for Reliable Thermal Feedback during In Vivo Tumor Therapy. Advanced Functional Materials, 2020, 30, 2002730.	14.9	73
18	Real-time deep-tissue thermal sensing with sub-degree resolution by thermally improved Nd3+:LaF3 multifunctional nanoparticles. Journal of Luminescence, 2016, 175, 149-157.	3.1	71

#	Article	IF	CITATIONS
19	Normalized-lifetime thermal-lens method for the determination of luminescence quantum efficiency and thermo-optical coefficients: Application toNd3+-doped glasses. Physical Review B, 2006, 73, .	3.2	70
20	Spectroscopic properties of Er ³⁺ -doped lead phosphate glasses for photonic application. Journal Physics D: Applied Physics, 2010, 43, 025102.	2.8	70
21	Optimizing and calibrating a mode-mismatched thermal lens experiment for low absorption measurement. Journal of the Optical Society of America B: Optical Physics, 2006, 23, 1408.	2.1	69
22	Pump-power-controlled luminescence switching in Yb3+â^•Tm3+ codoped water-free low silica calcium aluminosilicate glasses. Applied Physics Letters, 2007, 91, .	3.3	66
23	Core–shell rare-earth-doped nanostructures in biomedicine. Nanoscale, 2018, 10, 12935-12956.	5.6	63
24	Luminescent nanoprobes for thermal bio-sensing: Towards controlled photo-thermal therapies. Journal of Luminescence, 2016, 169, 394-399.	3.1	59
25	Visible–NIR emission and structural properties of Sm3+ doped heavy-metal oxide glass with composition B2O3–PbO–Bi2O3–GeO2. Journal of Luminescence, 2016, 171, 106-111.	3.1	58
26	Time-resolved thermal lens measurements of the thermo-optical properties of glasses at low temperature down to 20 K. Physical Review B, 2005, 71, .	3.2	56
27	Ultrafast photochemistry produces superbright short-wave infrared dots for low-dose in vivo imaging. Nature Communications, 2020, 11, 2933.	12.8	56
28	Concentration dependent luminescence and cross-relaxation energy transfers in Tb3+ doped fluoroborate glasses. Journal of Luminescence, 2019, 205, 282-286.	3.1	54
29	Femtosecond-laser-written, stress-induced Nd:YVO_4 waveguides preserving fluorescence and Raman gain. Optics Letters, 2010, 35, 916.	3.3	51
30	Ultrafast laser writing of optical waveguides in ceramic Yb:YAG: a study of thermal and non-thermal regimes. Applied Physics A: Materials Science and Processing, 2011, 104, 301-309.	2.3	47
31	Thermal lens spectroscopy of Nd:YAG. Applied Physics Letters, 2005, 86, 034104.	3.3	43
32	Ultrasensitive thermal lens spectroscopy of water. Optics Letters, 2009, 34, 1882.	3.3	41
33	Time resolved spectroscopy of infrared emitting Ag ₂ S nanocrystals for subcutaneous thermometry. Nanoscale, 2017, 9, 2505-2513.	5.6	41
34	Thermal effect on multiphonon-assisted anti-Stokes excited upconversion fluorescence emission in Yb 3+ -sensitized Er 3+ -doped optical fiber. Applied Physics B: Lasers and Optics, 2000, 70, 185-188.	2.2	40
35	Fluorescent nano-particles for multi-photon thermal sensing. Journal of Luminescence, 2013, 133, 249-253.	3.1	40
36	Continuous-wave diode-pumped Yb:glass laser with near 90% slope efficiency. Applied Physics Letters, 2006, 89, 121101.	3.3	39

#	Article	lF	CITATIONS
37	Thermally resistant waveguides fabricated in Nd:YAG ceramics by crossing femtosecond damage filaments. Optics Letters, 2010, 35, 330.	3.3	39
38	1.319 μm excited thulium doped nanoparticles for subtissue thermal sensing with deep penetration and high contrast imaging. Sensors and Actuators B: Chemical, 2017, 238, 525-531.	7.8	39
39	Thermal lens study of the OH[sup â^] influence on the fluorescence efficiency of Yb[sup 3+]-doped phosphate glasses. Applied Physics Letters, 2005, 86, 071911.	3.3	38
40	Upconversion effect on fluorescence quantum efficiency and heat generation in Nd3+-doped materials. Optics Express, 2005, 13, 2040.	3.4	37
41	Fluorescence quantum efficiency and Auger upconversion losses of the stoichiometric laser crystalNdAl3(BO3)4. Physical Review B, 2005, 72, .	3.2	36
42	White light upconversion emission and color tunability in Er3+/Tm3+/Yb3+ tri-doped YNbO4 phosphor. Journal of Luminescence, 2018, 204, 676-684.	3.1	35
43	Color tunability with temperature and pump intensity in Yb3+/Tm3+ codoped aluminosilicate glass under anti-Stokes excitation. Journal of Chemical Physics, 2010, 133, 034507.	3.0	34
44	Fourfold output power enhancement and threshold reduction through thermal effects in an Er^3+/Yb^3+-codoped optical fiber laser excited at 1064 µm. Optics Letters, 1999, 24, 1287.	3.3	32
45	Thulium doped LaF ₃ for nanothermometry operating over 1000 nm. Nanoscale, 2019, 11, 8864-8869.	5.6	31
46	Thermal effect on upconversion fluorescence emission in Er-doped chalcogenide glasses under anti-Stokes, Stokes and resonant excitation. Optical Materials, 2003, 22, 275-282.	3.6	30
47	The role of TiO2 in the B2O3–Na2O–PbO–Al2O3 glass system. Journal of Solid State Chemistry, 2011, 184, 3062-3065.	2.9	29
48	Thermal and Optical Properties of \${hbox {Yb}}^{3+}\$- and \${hbox {Nd}}^{3+}\$-Doped Phosphate Glasses Determined by Thermal Lens Technique. IEEE Journal of Quantum Electronics, 2007, 43, 751-757.	1.9	28
49	Luminescence and thermal lensing characterization of singly Eu3+ and Tm3+ doped Y2O3 transparent ceramics. Journal of Luminescence, 2015, 161, 306-312.	3.1	28
50	Thermal lens and heat generation of Nd:YAG lasers operating at 1.064 and 1.34 μm. Optics Express, 2008, 16, 6317.	3.4	27
51	Finite-size effect on the surface deformation thermal mirror method. Journal of the Optical Society of America B: Optical Physics, 2011, 28, 1735.	2.1	27
52	Optimum quantum dot size for highly efficient fluorescence bioimaging. Journal of Applied Physics, 2012, 111, 023513.	2.5	27
53	Influence of BaX2 (X = Cl, F) and Er2O3 concentration on the physical and optical properties of barium borate glasses. Physica B: Condensed Matter, 2019, 558, 146-153.	2.7	26
54	Microstructuration induced differences in the thermo-optical and luminescence properties of Nd:YAG fine grain ceramics and crystals. Journal of Chemical Physics, 2008, 129, 104705.	3.0	25

#	Article	IF	CITATIONS
55	Thermal lens study of energy transfer in Yb^3+/Tm^3+-co-doped glasses. Optics Express, 2007, 15, 9232.	3.4	24
56	Modeling the population lens effect in thermal lens spectrometry. Optics Letters, 2013, 38, 422.	3.3	24
57	Multichannel emission from Pr3+ doped heavy-metal oxide glass B2O3–PbO–GeO2–Bi2O3 for broadband signal amplification. Journal of Luminescence, 2016, 180, 341-347.	3.1	24
58	Energy transfer processes and heat generation in Yb[sup 3+]-doped phosphate glasses. Journal of Applied Physics, 2006, 100, 113103.	2.5	23
59	Effect of Nd3+ concentration quenching in highly doped lead lanthanum zirconate titanate transparent ferroelectric ceramics. Journal of Applied Physics, 2007, 101, 053111.	2.5	23
60	Luminescence and upconversion processes in <mml:math xmlns:mml="http://www.w3.org/1998/Math/MathML" altimg="si0041.gif" overflow="scroll"><mml:msup><mml:mrow><mml:mi>Er</mml:mi></mml:mrow><mml:mrow><mml:mn>3tellurite glasses. Journal of Luminescence, 2018, 201, 110-114.</mml:mn></mml:mrow></mml:msup></mml:math 	l:mn> <mr< td=""><td>nl:mo>+</td></mr<>	nl:mo>+
61	Spectroscopic properties of B2O3–PbO–Bi2O3–GeO2 glass doped with Sm3+ and gold nanoparticles. Optical Materials, 2016, 52, 230-236.	3.6	22
62	Energy transfer upconversion determination by thermal-lens and Z-scan techniques in Nd^3+-doped laser materials. Journal of the Optical Society of America B: Optical Physics, 2009, 26, 1002.	2.1	21
63	Multicolor Upconversion Emission and Color Tunability in Tm3+/Er3+/Yb3+ Tri-Doped NaNbO3 Nanocrystals. Materials Express, 2012, 2, 294-302.	0.5	21
64	Thermal lens spectrometry in pyroelectric lithium niobate crystals. Applied Physics B: Lasers and Optics, 2008, 93, 879-883.	2.2	20
65	Tunable light emission mediated by energy transfer in Tm3+/Dy3+ co-doped LaF3 nanocrystals under UV excitation. Journal of Luminescence, 2017, 188, 18-23.	3.1	19
66	Two Photon Thermal Sensing in Er ³⁺ /Yb ³⁺ Co-Doped Nanocrystalline NaNbO ₃ . Journal of Nanoscience and Nanotechnology, 2013, 13, 6841-6845.	0.9	18
67	1.319 μm excited intense 800 nm frequency upconversion emission in Tm3+-doped fluorogermanate g Applied Physics Letters, 2015, 107, 211103.	glass.	17
68	IR-to-visible frequency upconversion in Yb3+/Tm3+ co-doped phosphate glass. Optical Materials, 2017, 73, 1-6.	3.6	17
69	Near-infrared quantum cutting in Pr3+/Yb3+ NaYF4 nanocrystals for luminescent solar converter. Journal of Luminescence, 2021, 233, 117919.	3.1	17
70	Luminescent and thermo-optical properties of Nd3+-doped yttrium aluminoborate laser glasses. Journal of Applied Physics, 2009, 106, .	2.5	16
71	Synthesis and spectroscopic characterization of a fluorescent pyrrole derivative containing electron acceptor and donor groups. Spectrochimica Acta - Part A: Molecular and Biomolecular Spectroscopy, 2014, 128, 812-818.	3.9	16
72	Luminescence dynamics in Eu3+ doped fluoroborate glasses. Journal of Luminescence, 2017, 192, 827-831.	3.1	15

#	Article	IF	CITATIONS
73	Synthesis and characterization of Ag ₂ S and Ag ₂ S/Ag ₂ (S,Se) NIR nanocrystals. Nanoscale, 2019, 11, 9194-9200.	5.6	15
74	Thermal lens spectroscopy through phase transition in neodymium doped strontium barium niobate laser crystals. Journal of Applied Physics, 2007, 101, 023113.	2.5	14
75	Highly efficient upconversion emission and luminescence switching from Yb3+/Tm3+ co-doped water-free low silica calcium aluminosilicate glass. Journal of Luminescence, 2008, 128, 744-746.	3.1	14
76	Thermal mirror spectrometry: An experimental investigation of optical glasses. Optical Materials, 2013, 35, 1129-1133.	3.6	14
77	Three- and two-photon upconversion luminescence switching in Tm3+/Yb3+-codoped sodium niobate nanophosphor. Journal of Nanophotonics, 2014, 8, 083093.	1.0	14
78	Luminescent anti-reflection coatings based on Er3+ doped forsterite for commercial silicon solar cells applications. Solar Energy, 2018, 170, 752-761.	6.1	14
79	Nd3+ doped TiO2 nanocrystals as self-referenced optical nanothermometer operating within the biological windows. Sensors and Actuators A: Physical, 2021, 317, 112445.	4.1	14
80	Quantum efficiencies and thermo-optical properties of Er3+-, Nd3+-, and Pr3+-single doped lead-indium-phosphate glasses. Journal of Applied Physics, 2009, 106, .	2.5	13
81	Photothermal Study of Two Different Nanofluids Containing SiO2 and TiO2 Semiconductor Nanoparticles. International Journal of Thermophysics, 2012, 33, 69-79.	2.1	13
82	Resonant excited state absorption and relaxation mechanisms in Tb^3+-doped calcium aluminosilicate glasses: an investigation by thermal mirror spectroscopy. Optics Letters, 2013, 38, 4667.	3.3	13
83	Second-order nonlinearity of NaNbO3 nanocrystals with orthorhombic crystalline structure. Journal of Luminescence, 2019, 211, 121-126.	3.1	13
84	Nystatin complexation with <mml:math <br="" xmlns:mml="http://www.w3.org/1998/Math/MathML">display="inline" id="d1e478" altimg="si26.svg"><mml:mi>l^2</mml:mi></mml:math> -cyclodextrin: Spectroscopic evaluation of inclusion by FT-Raman, photoacoustic spectroscopy, andA1H NMR. Materials Chemistry and Physics, 2020, 239, 122117.	4.0	13
85	Thermal lens and Auger upconversion losses' effect on the efficiency of Nd^3+-doped lead lanthanum zirconate titanate transparent ceramics. Journal of the Optical Society of America B: Optical Physics, 2006, 23, 2097.	2.1	12
86	Time-resolved study electronic and thermal contributions to the nonlinear refractive index of Nd3+:SBN laser crystals. Journal of Luminescence, 2008, 128, 1013-1015.	3.1	12
87	Time resolved thermal lens measurements of the thermo-optical properties of Nd2O3-doped low silica calcium aluminosilicate glasses down to 4.3K. Journal of Non-Crystalline Solids, 2008, 354, 574-579.	3.1	12
88	Giant sensitivity of an optical nanothermometer based on parametric and non-parametric emissions from Tm3+ doped NaNbO3 nanocrystals. Journal of Luminescence, 2020, 226, 117475.	3.1	12
89	Spectral studies of highly Dy3+ doped PbO–ZnO–B2O3–P2O5 glasses. Journal of Luminescence, 2021, 231, 117839.	3.1	12
90	Auger upconversion energy transfer losses and efficient 1.06Âμm laser emission in Nd3+ doped fluoroindogallate glass. Applied Physics B: Lasers and Optics, 2006, 83, 565-569.	2.2	11

#	Article	IF	CITATIONS
91	Nonlinear refraction and absorption through phase transition in a Nd:SBN laser crystal. Physical Review B, 2009, 79, .	3.2	11
92	Thermal lens study of thermo-optical properties and concentration quenching of Er3+-doped lead pyrophosphate-based glasses. Journal of Applied Physics, 2012, 111, .	2.5	11
93	UV–visible-NIR light generation through frequency upconversion in Tm3+-doped low silica calcium aluminosilicate glasses using multiple excitation around 1.2†µm. Journal of Solid State Chemistry, 2018, 260, 147-150.	2.9	10
94	Optimizing the Nd:YF3 phosphor by impurities control in the synthesis procedure. Journal of Luminescence, 2018, 201, 156-162.	3.1	10
95	Cooperative Upconversion, Radiation Trapping, and Self-Quenching Effects in Highly Yb ³ ⁺ -Doped Oxyfluoride Glasses. Science of Advanced Materials, 2013, 5, 1948-1953.	0.7	10
96	Temperature triggering a photon-avalanche-like mechanism in NdAl3(BO3)4 particles under excitation at 1064Ânm. Journal of Luminescence, 2021, , 118645.	3.1	10
97	Thermal properties of barium titanium borate glasses measured by thermal lens technique. Journal of Non-Crystalline Solids, 2006, 352, 3577-3581.	3.1	9
98	Optical distortions through phase transition in the Nd3+:SBN laser crystal. Applied Physics Letters, 2006, 88, 161116.	3.3	9
99	Spectroscopic investigation and heat generation of Yb^3+/Ho^3+ codoped aluminosilicate glasses looking for the emission at 2Âμm. Journal of the Optical Society of America B: Optical Physics, 2013, 30, 1322.	2.1	9
100	Non-isothermal crystallization of TeO2-Na2O-TiO2 glasses. Journal of Non-Crystalline Solids, 2019, 524, 119655.	3.1	9
101	A generalized Drude–Lorentz model for refractive index behavior of tellurite glasses. Journal of Materials Science: Materials in Electronics, 2019, 30, 16949-16955.	2.2	9
102	Random laser and stimulated Raman scattering in liquid solutions of rhodamine dyes. Laser Physics Letters, 2019, 16, 055002.	1.4	9
103	Role of heat treatment on the structural and luminescence properties of Yb ³⁺ /Ln ³⁺ (Ln = Tm, Ho and Er) co-doped LaF ₃ nanoparticles. Physical Chemistry Chemical Physics, 2020, 22, 24535-24543.	2.8	9
104	White light source and optical thermometry based on zinc-tellurite glass tri-doped with Tm3+/Er3+/Sm3+. Journal of Alloys and Compounds, 2022, 899, 163305.	5.5	9
105	Time-resolved mirage method: A three-dimensional theory and experiments. Journal of Applied Physics, 2012, 111, 093502.	2.5	8
106	Response to "Critical Growth Temperature of Aqueous CdTe Quantum Dots is Nonâ€negligible for their Application as Nanothermometers― Small, 2013, 9, 3198-3200.	10.0	8
107	Generation of multiwavelength light in the region of the biological windows in Tm3+-doped fiber excited at 1.064 μm. Applied Physics Letters, 2016, 109, 261108.	3.3	8
108	Thermal lens and interferometric method for glass transition and thermo physical properties measurements in Nd_2O_3 doped sodium zincborate glass. Optics Express, 2008, 16, 21248.	3.4	7

#	ARTICLE	IF	CITATIONS
109	Luminescence Quantum Efficiency of \${m Nd}^{3+}{colon}{m Y}_{3}{m Al}_{5}{m O}_{12}\$ Garnet Laser Ceramics Determined by Pump-Induced Line Broadening. IEEE Journal of Quantum Electronics, 2010, 46, 1870-1876.	1.9	7
110	Thermo-optical characteristics and concentration quenching effects in Nd3+doped yttrium calcium borate glasses. Journal of Chemical Physics, 2011, 134, 124503.	3.0	7
111	Thermo-optical and spectroscopic properties of Nd:YAG fine grain ceramics: towards a better performance than the Nd:YAG laser crystals. Laser Physics Letters, 2016, 13, 025004.	1.4	7
112	Determination of fluorescence quantum efficiency in solutions by thermal lens measurements at several wavelengths: Application to Rhodamine 6G. European Physical Journal Special Topics, 2005, 125, 225-227.	0.2	6
113	Influence of temperature and excitation procedure on the athermal behavior of Nd3+-doped phosphate glass: Thermal lens, interferometric, and calorimetric measurements. Journal of Applied Physics, 2009, 106, .	2.5	6
114	Influence of the Al concentration on the electronic properties of coupled and uncoupled AlxGa1â^'xAs/AlAs/AlyGa1â^'yAs double quantum wells. Physica E: Low-Dimensional Systems and Nanostructures, 2014, 61, 158-166.	2.7	6
115	Magnetic upconverting fluorescent NaGdF4:Ln3+ and iron-oxide@NaGdF4:Ln3+ nanoparticles. AIP Advances, 2018, 8, 056710.	1.3	6
116	Optical nanothermometry under multiphonon assisted anti-Stokes excitation operating in the biological windows. Sensors and Actuators A: Physical, 2019, 296, 375-382.	4.1	6
117	Interaction between Yb3+ doped glasses substrates and graphene layers by raman spectroscopy. Thin Solid Films, 2020, 712, 138315.	1.8	6
118	Thermoelastic properties across martensitic transformation of Ni <mml:math xmlns:mml="http://www.w3.org/1998/Math/MathML" display="inline" id="d1e134" altimg="si4.svg"><mml:msub><mml:mrow /><mml:mrow><mml:mn>2</mml:mn></mml:mrow></mml:mrow </mml:msub>MnGa Heusler alloy from</mml:math 	2.7	6
119	time-resolved photothermal mirror. Physica B: Condensed Matter, 2021, 605, 412713. Evaluation of thermo-optical properties of poly(2-methoxyaniline) solutions. Chemical Physics Letters, 2007, 442, 400-404.	2.6	5
120	Insight into dual-modality of triply doped magnetic-luminescent iron-oxide/NaGdF4:RE3+ (RE =â€⁻Ce, Tb, Dy) nanoparticles. Materials Letters, 2018, 213, 358-361.	2.6	5
121	High-sensitivity absorption coefficients measurements using thermal lens spectrometry. European Physical Journal Special Topics, 2005, 125, 229-232.	0.2	4
122	Direct measurement of photo-induced nanoscale surface displacement in solids using atomic force microscopy. Optical Materials, 2015, 48, 71-74.	3.6	4
123	Roles of fluorine and annealing on optical and structural properties of Nd:YF3 phosphor. Journal of Luminescence, 2016, 175, 237-242.	3.1	4
124	Vis–NIR luminescence emission via energy-transfer in Tm 3+ /Er 3+ and Tm 3+ /Nd 3+ codoped glass under 1.319 µm excitation. Journal of Luminescence, 2016, 172, 275-278.	3.1	4
125	Binary activated iron oxide/SiO ₂ /NaGdF ₄ :RE (RE = Ce, and Eu; Yb, and Er) nanoparticles: synthesis, characterization and their potential for dual <i>T</i> ₁ – <i>T</i> ₂ weighted imaging. New Journal of Chemistry, 2020, 44, 832-844.	2.8	4
126	Enhanced thermometry parameters in Er3+-doped zinc tellurite glasses containing silver nanoparticles. Optik, 2021, 240, 166929.	2.9	4

#	Article	IF	CITATIONS
127	Effect of Gold Nanoparticles and Unwanted Residues on Raman Spectra of Graphene Sheets. Brazilian Journal of Physics, 2018, 48, 477-484.	1.4	3
128	3Dâ€Printed Acoustofluidic Devices for Raman Spectroscopy of Cells. Advanced Engineering Materials, 2021, 23, 2100552.	3.5	3
129	Fluorescence quantum efficiency in Nd ₂ O ₃ -doped aluminosilicate glasses by multiwavelength thermal lens method. European Physical Journal Special Topics, 2005, 125, 185-187.	0.2	3
130	<title>Refractive index changes in solid-state laser materials</title> ., 2006, , .		2
131	Temperature dependence of the thermophysical properties of Neodymium doped borate glasses. Optical Materials, 2011, 33, 1563-1568.	3.6	2
132	Modeling population and thermal lenses in the presence of Auger Upconversion for Nd^3+ doped materials. Optics Express, 2015, 23, 15983.	3.4	2
133	Generation of Vis-NIR light within the first biological optical window via frequency upconversion in Tm3+- and Tm3+/Er3+-doped tellurite glass excited at 1319 nm. , 2016, , .		1
134	Multicolor light emission in Dy ³⁺ /Tb ³⁺ -codoped LaF ₃ nanocrystals under UV excitation. Optical Engineering, 2017, 56, 047101.	1.0	1
135	Facile and fast synthesis of lanthanide nanoparticles for bio-applications. , 2020, , 195-228.		1
136	Energy conversion dynamics of novel lanthanide-doped forsterite photoactive devices. Applied Surface Science, 2021, 561, 150059.	6.1	1
137	3Dâ€Printed Acoustofluidic Devices for Raman Spectroscopy of Cells. Advanced Engineering Materials, 2021, 23, 2170040.	3.5	1
138	Ultra-sensitive thermal lens spectroscopy of water. , 2009, , .		0
139	Efficient 800nm upconversion luminescence emission in 1.319μm excited thulium-doped fluorogermanate. , 2016, , .		0
140	Optical Sensing Based on Rare-Earth-Doped Tellurite Glasses. , 2018, , 179-201.		0
141	Spectroscopic properties and heat generation of Yb3+/Ho3+ and Tm3+/Ho3+ co-doped low silica calcium aluminosilicate glasses for emission around 2 ŵm. , 2012, , .		0